Neurology®
The most widely read and highly cited peer-reviewed neurology journal
The Official Journal of the American Academy of Neurology

AMERICAN ACADEMY OF NEUROLOGY®

Neurology Publish Ahead of Print
DOI: 10.1212/WNL.0000000000200142

Cerebral Microbleeds, Cerebral Amyloid Angiopathy, and Their Relationships to Quantitative Markers of Neurodegeneration

Author(s):
Charles Beaman, MD/PhD[1,2]; Krystyna Kozii, MD[1]; Saima Hilal, MD/PhD[3,4,5]; Minghua Liu, PhD[1]; Anthony J Spagnolo-Allende, MD/MPH[1]; Guillermo Polanco-Serra, BS[6]; Christopher Chen, MD[3,4]; Ching-Yu Cheng, MD/MPH/PhD[7,8]; Daniela Zambrano, MD[1]; Burak Arikan, MD[9]; Victor J. Del Brutto, MD[10]; Clinton Wright, MD/MS[11]; Xena E. Flowers, BS[12]; Sandra P. Leskinen, MA[12]; Tatjana Rundek, MD/PhD[10]; Amanda Mitchell, BA[1]; Jean Paul Vonsattel, MD[12]; Etty Cortes, MD[13]; Andrew F. Teich, MD[1,12]; Ralph L. Sacco, MD/MS[10]; Mitchell S. V. Elkind, MD[1,14]; David Roh, MD[1]; Jose Gutierrez, MD/MPH[1] on behalf of for the Alzheimer's Disease Neuroimaging Initiative*

Corresponding Author:
Jose Gutierrez, jg3233@cumc.columbia.edu

Affiliation Information for All Authors: Charles Beaman, MD/PhD1, 2; Krystyna Kozii, MD1; Saima Hilal, MD/PhD3, 4, 5; Minghua Liu, PhD1; Anthony J Spagnolo-Allende, MD/MPH1; Guillermo Polanco-Serra, BS6; Christopher Chen, MD3,4; Ching-Yu Cheng, MD/MPH/PhD7,8; Daniela Zambrano, MD1; Burak Arikan, MD9; Victor J. Del Brutto, MD10; Clinton Wright, MD/MS11; Xena E. Flowers, BS12; Sandra P. Leskinen, MA12; Tatjana Rundek, MD/PhD10; Amanda Mitchell, BA1; Jean Paul Vonsattel, MD12; Etty Cortes, MD13; Andrew F. Teich, MD1, 12; Ralph L. Sacco, MD/MS10; Mitchell SV Elkind, MD/MS1, 14; David Roh, MD1; Jose Gutierrez, MD/MPH1, for the Alzheimer's Disease Neuroimaging Initiative* 1 Department of Neurology, Columbia University Irving Medical Center, New York, NY; 2 Department of Neurology, UCLA Medical Center, Los Angeles, CA; 3 Memory Aging and Cognition Center, National University Health System, Singapore; 4 Department of Pharmacology, Yong Loo Lin School of Medicine, National University of Singapore, Singapore; 5 Saw Swee Hock School of Public Health, National University of Singapore and National University Health System, Singapore; 6 College of Medicine, SUNY Upstate Medical University, Syracuse, NY; 7 Singapore Eye Research Institute, Singapore National Eye Centre, Singapore; 8 Ophthalmology and Visual Sciences Academic Clinical Program, Duke-NUS Medical School, National University of Singapore, Singapore; 9 Istanbul University Cerrahpasa School of Medicine, Istanbul, Turkey;; 10 Department of Neurology and Evelyn F. McKnight Brain Institute, Miller School of Medicine, University of Miami Miller School of Medicine, Miami, FL; 11 National Institute of Health, Bethesda, MD; 12 Department of Pathology and Cell Biology, Columbia University Irving Medical Center, New York, NY; 13 Department of Pathology, Icahn School of Medicine at Mount Sinai, New York, NY; 14 Department of Epidemiology, Mailman School of Public Health, Columbia University, New York, NY

Equal Author Contribution:

*Data used in preparation of this article were obtained from the Alzheimer's Disease Neuroimaging Initiative (ADNI) database (adni.loni.usc.edu). As such, the investigators within the ADNI contributed to the design and implementation of ADNI and/or provided data but did not participate in analysis or writing of this report. A complete listing of ADNI investigators can be found in Appendix 2 at [insert SDC link].

Contributions:

Charles Beaman: Drafting/revision of the manuscript for content, including medical writing for content; Major role in the acquisition of data; Study concept or design; Analysis or intepretation of data
Krystyna Kozii: Major role in the acquisition of data
Saima Hilal: Drafting/revision of the manuscript for content, including medical writing for content; Major role in the acquisition of data
Minghua Liu: Drafting/revision of the manuscript for content, including medical writing for content; Analysis or intepretation of data
Anthony J Spagnolo-Allende: Drafting/revision of the manuscript for content, including medical writing for content; Analysis or intepretation of data
Guillermo Polanco-Serra: Major role in the acquisition of data
Christopher Chen: Drafting/revision of the manuscript for content, including medical writing for content; Major role in the acquisition of data
Ching-Yu Cheng: Drafting/revision of the manuscript for content, including medical writing for content; Major role in the acquisition of data
Daniela Zambrano: Drafting/revision of the manuscript for content, including medical writing for content; Major role in the acquisition of data
Burak Arikan: Major role in the acquisition of data
Victor J. Del Brutto: Drafting/revision of the manuscript for content, including medical writing for content; Major role in the acquisition of data
Clinton Wright: Drafting/revision of the manuscript for content, including medical writing for content
Xena E. Flowers: Major role in the acquisition of data
Sandra P. Leskinen: Major role in the acquisition of data
Tatjana Rundek: Drafting/revision of the manuscript for content, including medical writing for content; Major role in the acquisition of data
Amanda Mitchell: Major role in the acquisition of data
Jean Paul Vonsattel: Drafting/revision of the manuscript for content, including medical writing for content; Major role in the acquisition of data
Etty Cortes: Drafting/revision of the manuscript for content, including medical writing for content; Major role in the acquisition of data
Andrew F. Teich: Drafting/revision of the manuscript for content, including medical writing for content; Major role in the acquisition of data
Ralph L. Sacco: Drafting/revision of the manuscript for content, including medical writing for content; Major role in the

acquisition of data
Mitchell S. V. Elkind: Drafting/revision of the manuscript for content, including medical writing for content; Major role in the acquisition of data
David Roh: Drafting/revision of the manuscript for content, including medical writing for content
Jose Gutierrez: Drafting/revision of the manuscript for content, including medical writing for content; Major role in the acquisition of data; Study concept or design; Analysis or intepretation of data

Figure Count:
4

Table Count:
3

Search Terms:
[2] All Cerebrovascular disease/Stroke, [7] Intracerebral hemorrhage, [13] Other cerebrovascular disease/ Stroke, [32] Vascular dementia, Cerebral Amyloid Angiopathy

Acknowledgment:
Data collection and sharing for this project was funded by the Alzheimer's Disease Neuroimaging Initiative (ADNI) (National Institutes of Health Grant U01 AG024904) and DOD ADNI (Department of Defense award number W81XWH-12-2-0012). ADNI is funded by the National Institute on Aging, the National Institute of Biomedical Imaging and Bioengineering, and through generous contributions from the following: AbbVie, AlzheimerÂ's Association; Alzheimer's Drug Discovery Foundation; Araclon Biotech; BioClinica, Inc.; Biogen; Bristol-Myers Squibb Company; CereSpir, Inc.; Cogstate; Eisai Inc.; Elan Pharmaceuticals, Inc.; Eli Lilly and Company; EuroImmun; F. Hoffmann-La Roche Ltd and its affiliated company Genentech, Inc.; Fujirebio; GE Healthcare; IXICO Ltd.; Janssen Alzheimer Immunotherapy Research & Development, LLC.; Johnson & Johnson Pharmaceutical Research & Development LLC.; Lumosity; Lundbeck; Merck & Co., Inc.; Meso Scale Diagnostics, LLC.; NeuroRx Research; Neurotrack Technologies; Novartis Pharmaceuticals Corporation; Pfizer Inc.; Piramal Imaging; Servier; Takeda Pharmaceutical Company; and Transition Therapeutics. The Canadian Institutes of Health Research is providing funds to support ADNI clinical sites in Canada. Private sector contributions are facilitated by the Foundation for the National Institutes of Health (www.fnih.org). The grantee organization is the Northern California Institute for Research and Education, and the study is coordinated by the Alzheimer's Therapeutic Research Institute at the University of Southern California. ADNI data are disseminated by the Laboratory for Neuro Imaging at the University of Southern California.

Study Funding:
JG: R01 AG057709 & R01AG066162; CBB: NIH/NINDS R25 NS070697; RLS, ME: NIH/NINDS R0129993; GPS: T35AG044303.

Disclosures:
M. Elkind receives outside the submitted work, study drug in kind from the BMS-Pfizer Alliance for Eliquis® and ancillary research funding but no personal compensation for an NIH-funded trial of stroke prevention in patients with cryptogenic stroke, and royalties from UpToDate for chapters on stroke. R. L. Sacco discloses personal compensation from the American Heart Association for Editor-In-Chief of Stroke. The remaining authors report no disclosures relevant to the manuscript.

Handling Editor Statement:

ABSTRACT:

Background: Age-related cognitive impairment is driven by the complex interplay of neurovascular and neurodegenerative disease. There is a strong relationship between cerebral microbleeds (CMBs), cerebral amyloid angiopathy (CAA), and the cognitive decline observed in conditions such as Alzheimer's disease. However, in the early, preclinical phase of cognitive impairment, the extent to which CMBs and underlying CAA impact volumetric changes in the brain related to neurodegenerative disease remains unclear.

Methods: We performed cross-sectional analyses from 3 large cohorts: The Northern Manhattan Study (NOMAS), Alzheimer's Disease Neuroimaging Initiative (ADNI), and the Epidemiology of Dementia in Singapore study (EDIS). We conducted a confirmatory analysis of 82 autopsied cases from the Brain Arterial Remodeling Study (BARS). We implemented multivariate regression analyses to study the association between two related markers of cerebrovascular disease – MRI-based CMBs and autopsy-based CAA, as independent variables, and volumetric markers of neurodegeneration, as dependent variables. NOMAS included mostly dementia-free participants aged 55 years or older from Northern Manhattan. ADNI included participants living in the United States aged 55-90 years with a range of cognitive status. EDIS included community-based participants living in Singapore aged 60 years and older with a range of cognitive status. The BARS included post-mortem pathological samples.

Results: We included 2657 participants with available MRI data and 82 autopsy cases from the BARS. In a meta-analysis of NOMAS, ADNI and EDIS, superficial CMBs were associated with larger gray ($\beta=4.49 \pm 1.13$, $P=0.04$) and white ($\beta=4.72 \pm 2.1$, $P=0.03$) matter volumes. The association between superficial CMBs and larger white matter volume was more evident in participants with one CMB ($\beta=5.17 \pm 2.47$, $P=0.04$) than in those with ≥ 2 CMBs ($\beta=1.97 \pm 3.41$, $P=0.56$). In the BARS, CAA was associated with increased cortical thickness ($\beta = 6.5 \pm 2.3$, $P=0.016$) but not with increased brain weight ($\beta=1.54 \pm 1.29$, $P=0.26$).

Discussion: Superficial CMBs are associated with larger morphometric brain measures, specifically white matter volume. This association is strongest in brains with fewer CMBs, suggesting that the CMBs/CAA contribution to neurodegeneration may not relate to tissue loss, at least in early stages of disease.

INTRODUCTION:

Age-related cognitive decline is driven by the complex interactive effects of neurovascular and neurodegenerative disease.[1, 2] This interplay is well illustrated by cerebral microbleeds (CMBs), which are small, round collections of hemosiderin-laden macrophages that represent foci of prior microhemorrhages in the brain.[3] CMBs located in deep brain regions (e.g. basal ganglia and infratentorial regions) represent radiological biomarkers for small-vessel vascular disease and are associated with risk factors such as hypertension, hyperlipidemia, and diabetes.[4, 5] Conversely, CMBs in superficial (or lobar) regions of the brain are pathologically characterized by the gradual deposition of β-amyloid (Aβ) in vessel walls, known as cerebral amyloid angiopathy (CAA).[6, 7] CAA is a clinical entity characterized by older age, disseminated superficial siderosis, macrobleeds, and multiple CMBs in the lobar regions of the brain.[8] The relationship between CMBs, CAA, and cognitive decline is complex but a strong association has emerged in recent years. CMBs are present in approximately 20% of older individuals with normal cognition but up to 40% of people with Alzheimer's disease (AD).[9] Importantly, there is a significant association between CMBs and increased cognitive impairment and mortality.[10-13] CAA and AD also overlap – both involve the aberrant deposition of Aβ, and an estimated 52–98% of individuals with AD neuropathologic changes also have CAA.[14]

The structural hallmark of many neurodegenerative diseases such as AD is progressive cortical atrophy.[15] Previous work has indicated that brain atrophy may also be a key neuroimaging marker of neurovascular disease.[16] Small vessel disease, for example, is characterized on MRI imaging by white matter hyperintensities, dilated perivascular spaces (PVS), lacunar infarcts and CMBs, but these distinct markers are thought to ultimately coalesce into brain atrophy as the final common pathway.[17] Additionally, one prior study demonstrated that people with both hereditary and sporadic CAA have decreased cortical thickness compared to age-matched healthy controls.[18] Although superficial CMBs are strongly linked to underlying CAA pathology, there are conflicting reports regarding the association of superficial CMBs and gray matter volume, with two recent studies finding no association[18, 19] and one study finding superficial CMBs to be associated with smaller gray matter volumes.[20] Prior work has also shown similarly

conflicting evidence regarding the relationship between superficial CMBs/CAA and white matter volume.[19, 21]

In light of these discrepancies, we attempted to elucidate how CMBs relate to morphological changes in the brain (supratentorial brain volume, gray and white matter volumes and cortical thickness) while accounting for other markers of small vessel disease. Leveraging three population samples with available brain MRI and a collection of autopsied brains, we hypothesized that superficial CMBs and related CAA are associated with volumetric parameters of neurodegeneration.

MATERIAL & METHODS:

Standard Protocol Approvals, Registrations, and Patient Consents:

The Institutional Review Boards and ethical standards committees at each participating institution approved of the study protocol, including participant data collection and subsequent publication of data related to each cohort. Written informed participant consent was obtained prior to participation in the study.

Cohort Participants:

Northern Manhattan Study (NOMAS):

NOMAS is an observational, prospective, population-based cohort of stroke-free participants enrolled in Northern Manhattan that started in 1993. From 2003 to 2008, stroke-free participants 55 years or older were invited to undergo a brain MRI. Detailed descriptions of inclusion and exclusion criteria for the NOMAS cohort and MRI sub-study were previously published.[22, 23] Subjects were not categorized by cognitive ability but were estimated to be dementia-free. In NOMAS, baseline demographic and clinical characteristics were either self-reported, obtained from prescribed medications, or obtained from blood pressure/laboratory evidence, as previously described.[24] Smoking was defined as self-reported current smoking at the time of MR imaging.

Alzheimer's Disease Neuroimaging Initiative (ADNI):

Data used in the preparation of this article were obtained from the ADNI database (adni.loni.usc.edu). The ADNI was launched in 2003 as a public-private partnership, led by

Principal Investigator Michael W. Weiner, MD. The primary goal of ADNI has been to test whether serial magnetic resonance imaging (MRI), positron emission tomography (PET), other biological markers, and clinical and neuropsychological assessment can be combined to measure the progression of mild cognitive impairment (MCI) and early Alzheimer's disease (AD). ADNI included subjects aged 55-90.[25] Full inclusion/exclusion criteria are described in detail at www.adni-info.org. Briefly, the cohort included subjects classified as cognitively normal, mild cognitive impairment, and AD.[26] Clinical characteristics including hypertension, diabetes, hypercholesterolemia, and smoking status were obtained during a baseline visit using standardized measurements and medications.[25] We included a subset of ADNI who underwent 3T brain MRI from June 2010 until March 2012.

The Epidemiology of Dementia in Singapore study (EDIS):
EDIS is a subsample of a population-based cohort of Chinese, Malay, and Indian subjects aged 60 years and older. Participants were included if they screened positive with the Abbreviated Mental Test or a self-reported history of forgetfulness, as previously described.[27] In EDIS, vascular risk factors were obtained from standardized recordings, laboratory values, or use of medications for hypertension, diabetes, and hyperlipidemia. Smoking was categorized as never-smokers and any smoking history (past and current smokers).[27] We analyzed the subset of participants that underwent 3T MRI brain imaging and had available *Apoe4* genotype.

The Brain Arterial Remodeling Study (BARS) is a collection of over 300 Circle of Willis samples obtained at autopsy in various brain banks. Detailed descriptions of pathological processing were previously described.[28, 29] More recently, we started adding brain samples corresponding to the Circle of Willis of the New York Presbyterian Brain Bank as an extension of the investigation of the brain arterial remodeling role in neurodegeneration.

The study size for the cross-sectional analyses was based on the subject-level eligibility based on the inclusion and exclusion criteria for each respective cohort.

MRI Examination:

NOMAS imaging was performed on a dedicated 1.5-T research MRI system (Philips Medical Systems). CMBs were manually counted using T2* gradient echo (GRE) sequences in the coronal plane, using the Brain Observer MicroBleed Scale, as previously described.[30] Using T1 axial sequences, we obtained total supratentorial brain volume (excluding ventricles), total gray matter volume, total white matter volume, and cortical thickness. T1-weighted and FLAIR MRI sequences underwent motion correction, skull stripping, and transformation into Talaraich space.[31] Images were segmented, and gray and white matter boundaries were identified and underwent automated topology correction and surface deformation. To obtain total supratentorial brain volume, non-brain elements were manually removed by operator-guided tracing, as previously described.[32] Brain covert infarcts and dilated PVS were rated using a pathology-informed algorithm that aims at distinguishing infarcts from PVS using T1 and FLAIR sequences with a good reliability.[23] Volumes were obtained by adding brain voxels from the segmentation of T1-weighted images. We used the Freesurfer image analysis suite version 5.1 (https://surfer.nmr.mgh.harvard.edu/) to measure cortical thickness.[32]

ADNI imaging was conducted on 3-T MRI scanners at 54 different sites. A full description of MRI processing is available at http://adni.loni.usc.edu/methods/documents/mri-protocols/. Briefly, two radiologists used T2* GRE sequences to count CMBs as homogenous hypointense lesions up to 10 mm in diameter. The inter-rater agreement between the two radiologists on definite versus not-definite CMBs was 85%, which corresponded to good agreement (kappa=68%).[33] Brain infarct information was downloaded from the ADNI website and used for analyses as present versus absent. Dilated PVS were rated by us using the same method as in NOMAS applied directly to downloaded T1 and FLAIR images.[23]

EDIS imaging was performed on a 3-T MRI (Siemens Magnetom Trio Tim scanner), using a 32-channel head coil, at the Clinical Imaging Research Centre of the National University of Singapore.[27] CMBs (also imaged using T2* GRE sequences) were graded using the Brain Observer Microbleed Scale and were classified as lobar or deep microbleeds as dichotomous variables.[30] Brain infarcts were defined as hypointense lesions on T1-weighted images and hyperintense on T2-weighted images. Total intracranial volume was obtained using T1- and T2-weighted MRI images. Regional volumes were quantified using automatic segmentation, and a

model-based automated procedure (FreeSurfer version 5.1.0) was used to measure cortical thickness, as previously described.[27] Dilated PVS were quantified in four brain regions and the sum of these regions was used for this analysis. Information on dilated PVS was available only in EDIS participants of Chinese and Malay ancestry.

Post-mortem brain samples:

Cerebral hemispheres were fixed with 10 % buffered-formalin and coronally sectioned at 0.3 to 0.5 cm interval thickness. Samples were processed systematically as described elsewhere.[34] At least ten standardized anatomical sections were obtained and stained with Luxol/ hematoxylin & eosin (LHE) and submitted to β-amyloid (6E10; BioLegend; Catalog # 803003) immunohistochemistry (IHC). The IHC was performed by Ventana automated slide stainer without manual antigen retrieval and was detected using the Ventana ultraView universal DAB detection kit (Tucson, AZ) as recommended by the manufacturer. Each slide was digitized using a Leica SCN400 microscope with constant light at 40X magnification. Aperio Image Scope © Leica Biosystem Pathology Imaging (version 12.4.3.5008) was used for visualization and processing of images. In the slides for β-amyloid, we quantified the presence and number of vessels with β-amyloid deposits by dividing each brain slide into 10 two-dimensional boxes (40 μm^2 in size). For each box, we manually counted the number of vessels with β-amyloid deposits to quantify the burden of CAA. We also classified the location of each vessel with β-amyloid deposits into subcortical, cortical, or leptomeningeal (or extracortical) areas (Figure 1 A-D). The maximum number of CAA vessels per 40 μm^2 box was capped at 100. Cortical thickness was measured in slices of the brain surface. To account for the natural variation in cortical thickness observed in pathology given sulci folding, we measured the cortical thickness in at least five areas that visually appeared homogenous in thickness to obtain the average cortical thickness in a given brain section.

Statistical Analysis:

Analyses were initially carried out separately in each sample, and then combined in a meta-analysis. We assessed sample characteristics associated with any CMB in the three MRI cohorts and any CAA in the BARS using Fisher's exact and Student's t-tests, as indicated.

For the MRI samples, total brain, white and gray matter volumes were transformed into their logarithmic expression to approximate normality. Cortical thickness (in mm) was normally distributed. CMBs were expressed as a binary variable, segregated into lobar and deep, and ordinally as 0=no CMB, 1=one CMB, and 2=2 or more CMBs. We built generalized linear models with an identity link to obtain type 1 errors and beta estimates. Models were adjusted for age, sex, race/ethnicity, hypertension, diabetes, dyslipidemia, smoking, *Apoe4* status, prevalent chronic brain infarcts, head size, and white matter hyperintensity volume. In a post-hoc analysis, we also ran the same models adjusting additionally for dilated PVS in the three population cohorts. Due to differences in population origin and methodology, we carried out a meta-analysis and not pooled cohort analyses. We meta-analyzed the results of the three cohorts, and additionally ADNI and NOMAS separately, given their shared origin in the United States. RevMan 5.4 was used to perform all the meta-analyses (Review Manager (RevMan) [Computer program], Version 5.4, The Cochrane Collaboration, 2020.). A random effects model was carried out to calculate mean differences for continuous outcome data. Heterogeneity was assessed by two methods, the Q statistic test and the I^2 statistic test. For the Q statistic test, a P value ≤ 0.05 was considered statistically significant. For the I^2 statistic test, heterogeneity increased with a rising I^2 value. A fixed statistical model ($I^2 < 50\%$) or a random statistical model ($I^2 > 50\%$) was used according to the I^2 value.

In the BARS, we expressed CAA as present versus absent, and among those classified as present, the mean number of arteries with CAA per brain section. Due to limited availability of morphological measures in sectioned postmortem specimens, we only assessed brain weight and cortical thickness. Because of the two-level correlation in brain samples (number of arteries with CAA within each brain slice, and multiple brain slices per case), we built generalized linear mixed models adjusted for age, sex, race/ethnicity, hypertension, diabetes, dyslipidemia, smoking, and brain infarctions.

Statistical analyses were completed with SAS software (SAS version 9.4, Institute Inc., Cary, NC).

Data Availability:

Anonymized data not provided in the article because of space limitations may be shared at the request of any qualified investigator for purposes of replicating procedures and results.

Results:

a) Description of cohorts: We included 2657 participants with available data (918 from NOMAS, 1017 from ADNI, and 722 from EDIS) and 82 autopsy cases from the BARS. Baseline demographic characteristics of the samples are presented in Table 1.

The overall prevalence of CMBs was 6% in NOMAS, 22% in ADNI, and 31% in EDIS (Table 1). In the three cohorts, the prevalence of CMBs increased with age (Figure 2, eTable1). Stratifying CMBs by anatomical location shows a consistently higher prevalence of cortical CMBs compared to deep CMBs across the three cohorts (Figure 2).

In the BARS, the overall prevalence of CAA was 72% (23% purely cortical, 6% purely in the basal ganglia, and 43% mixed). CAA burden differed by anatomical region (Figure 3): the mean number of CAA vessels was highest in the lobar regions of the parietal (mean=7.4 ± 2.4) followed by occipital (mean=4.2 ± 1.5) and frontal (mean=4.2 ± 1.3) regions. Leptomeningeal (or extracortical) CAA was more prevalent in the occipital region (mean=3.8 ± 0.8), compared to the parietal (mean=3.6 ± 0.8) and frontal (mean=2.8 ± 0.6) regions. Subcortical/deep regions had the lowest amount of CAA, as observed in Figure 3.

b) Correlates of CMB/CAA: In a cross-sectional multivariate analysis, “any CMB” (collection of both superficial and deep CMBs) was associated with age across all three cohorts. The strength of association and statistical significance varied across cohorts for sex, ethnicity, vascular risk factors, *Apoe4* genotype and MRI markers of covert cerebrovascular disease (eTable 1).

c) Association of CMBs/CAA with cortical thickness and brain volumes: In each cohort, we assessed the relationship between CMBs and morphological brain metrics including total brain,

white matter, and gray matter volumes, in addition to cortical thickness (Table 2). In a meta-analysis of NOMAS, ADNI and EDIS, superficial CMBs were associated with larger gray (β=4.49 ± 1.13, P=0.04) and white (β=4.72 ± 2.1, P=0.03) matter volumes (Table 3). Stratifying by CMB severity, the association between superficial CMBs and larger white matter volume was more evident in participants with one CMB (β=5.17 ± 2.47, P=0.04) than in those with ≥ 2 CMBs (β=1.97 ± 3.41, P=0.56). The direction of associations was more consistent between ADNI and NOMAS than with EDIS (Table 2 and eFigures 1-4). We also found a positive correlation between superficial/deep CMBs and gray matter volumes (β=5.63 ± 1.27 and β=9.27 ± 3.52, P<0.05). CMBs were nominally associated with greater thickness (β=12.21 ± 7.72, P=0.10) only in NOMAS and ADNI meta-analyses. In post-hoc analyses, adding on dilated PVS scores in the three populations did not change the significance of the association between CMB and higher white matter volumes. Dilated PVS were independently associated with higher white matter volume in NOMAS (β=1.25 ± 0.59, P=0.04) and EDIS (β=0.35 ± 0.16, P=0.03), and nominally in the ADNI cohort (β=0.37 ± 0.47, P=0.43, eTable 2).

In the BARS, the two main outcomes were brain weight at autopsy and cortical thickness, and the main exposure was CAA expressed continuously as the mean number of vessels with CAA in each brain section of each cases. In a model adjusted for age, sex, demographics, vascular risk factors and presence of brain infarcts, CAA was associated with increased cortical thickness (β = 6.5 ± 2.3 µm, P=0.016) but not with increased brain weight (β=1.54 ± 1.29, P=0.26). We did not adjust for *Apoe*4 genotype because it was available only on a small subsample.

Discussion:

Growing evidence suggests that cognitive decline in the aging brain is driven by overlapping neurovascular and neurodegenerative disease. CAA and Alzheimer's disease pathological changes share a particularly close connection. Aβ underlies the pathogenesis of both conditions, and clinically, they frequently coexist and correlate in severity.[1, 14] CMBs are also more prevalent in AD compared to other forms of dementia.[10] To further investigate this interrelationship, we tested whether CMBs (and underlying CAA) correlate with key morphological markers of neurodegeneration. Contrary to our initial hypothesis, we found that lobar CMBs were independently associated with increased MRI-based total supratentorial brain

volume and white matter volume. We also found an unexpected significant association between autopsy-based CAA burden and increased cortical thickness. Prior work has demonstrated conflicting results regarding the relationship of CMBs and white matter volume. One recent study of memory clinic patients indicated that lobar CMBs, as opposed to deep microbleeds, were associated with reduced white matter volume.[35] However, in agreement with our findings, Wang and colleagues[19] studied a non-stroke, non-dementia population and found increased white matter volume in patients with lobar CMBs. One prior study examining cohorts of patients with hereditary cerebral hemorrhage with amyloidosis–Dutch type (HCHWA-D) and sporadic CAA provided evidence that CAA is associated with cortical atrophy, independent of AD.[18] We found consistent trends in the opposite association in our study of patients. This relationship was particularly notable in the American cohorts and the full study meta-analysis, but not in the Singaporean cohort. One reason for the discrepancy may be due to differences in baseline disease. That is, we observed significantly more CMBs in the Singaporean cohort compared to the American cohorts, which could suggest more advanced disease in the Singaporean cohort.[36] There may also be social or genetic differences between the cohorts that were not accounted for in our study. Importantly, we noted no difference in the proportion of *Apoe*4 mutations between the study groups.

In all three imaging cohorts, we found that CMBs were associated with older age, consistent with prior studies.[4, 5] Presumably, this relationship is due to weakened vessel walls and blood leakage into surrounding tissues seen with aging.[37] We found no association between CMBs and *Apoe*4 carrier status, despite previous work showing that individuals with the *Apoe*4 allele are more likely to have lobar microbleeds.[4] Our MRI populations did have a predominance of lobar compared to deep microbleeds, which was unanticipated given the high proportion of vascular risk factors, hypertension and hyperlipidemia, in each cohort. Research has indicated that a population with predominately lobar CMBs is likely to be associated with underlying amyloid angiopathy.[38] In agreement with prior work,[39, 40] we found a high proportion of CMBs in the frontal and parietal regions, and in pathological samples, we found more CAA in cortical regions compared to subcortical or deep regions of the brain. We also found a high proportion of CAA in leptomeningeal vessels and in the occipito-parietal lobar regions. CAA is thought to develop

from the posterior lobar regions to the anterior regions,[41] a progression that is associated with worsening executive function.[42]

The glymphatic system of the brain may help explain our unexpected results. The glymphatic system refers to paravascular flow of CSF to remove important interstitial waste solutes, such as Aβ.[43] This flux is driven by arterial pulsation and vasomotion and can be adversely affected by small vessel disease and stroke.[44-47] Pathologically, AD is characterized by the accumulation of neuritic plaques that result, at least in part, from dysfunctional clearance of Aβ in the glymphatic system. In CAA, Aβ accumulation in vessel walls is also likely the result of failure of intramural perivascular drainage.[48] These two overlapping pathologies are thought to create a feed-forward cycle, whereby increased vascular Aβ leads to decreased clearance of Aβ, worsening both CAA and AD.[2] Importantly, the combined interaction may represent a unifying therapeutic target to treat both conditions. It is clear from a large body of work that clinical dementia is associated with brain atrophy, but in the pre-clinical stages of disease, failure of the glymphatic system may lead to relative increase in interstitial fluid, which is reflected by increased brain morphometric measures, particularly white matter volume. Our finding of a significant relationship between dilated PVS and white matter volume may support this hypothesis. Future mechanistic studies are needed to assess whether larger brain volumes may be seen as a preclinical stage of Aβ deposition-related brain pathology.

The methodological strengths of this study include the large, ethnically diverse sample of participants, the clinical and imaging data, and the cross-validation of the analyses using autopsies, the gold-standard to diagnose CAA, in the BARS. The results of this study should be contextualized within certain limitations. First, in the three imaging cohorts, we assessed for CMBs, while in the BARS, we pathologically diagnosed CAA. We believe that the most likely cause of cortical CMBs is CAA, but prior work has indicated that CMBs and CAA don't perfectly overlap in the brain.[40] In addition, radiologic-histopathologic correlation studies indicate that the true-positive detection rate of CMBs ranges between 48%-89%, and false-positive mimics (including microdissections, microaneurysms, and microcalcifications) occur at a rate between 11%-24%.[3] Furthermore, up to 50% of CMBs are missed on MRI imaging compared to post-mortem analysis.[49] We also did not assess other radiological markers of CAA

such as superficial siderosis. A higher Tesla magnet would increase the sensitivity to detect CMBs and potentially yield closer results in the MRI and pathology cohorts. Failing to identify CMBs increases type 2 error. Therefore, we paid attention to the direction of associations in other morphometric brain measures to assess if more precise diagnosis of CMBs could result in greater statistical power. The precision of CAA diagnosis provided by pathology in the BARS may be the reason why in a smaller sample we were able to detect an association between CAA and cortical thickness.

Our study also has inherent limitations regarding its cross-sectional nature. In addition, the three cohorts differed in various respects that may have introduced selection biases. For instance, the NOMAS cohort was composed of mostly dementia-free participants while both ADNI and EDIS obtained patients with a range of cognitive ability. In NOMAS, participants were scanned with 1.5-T machines, while ADNI and EDIS implemented 3-T machines. The higher Tesla magnet may have identified a larger number of CMBs in a cognitively worse population to skew the associations. In addition, each study implemented T2* GRE sequences, which is less sensitive than susceptibility weighted imaging for the detection of CMBs.[50] Our models did adjust for a large range of clinical factors including age, sex, race/ethnicity, *Apoe4*, head size, prevalence of hypertension, diabetes, hypercholesterolemia, smoking, MRI evidence of infarction, and total white matter hyperintensity volume, but there may have been other unmeasured clinical factors for which we did not account. We also did not conduct morphological analyses on each specific cortical area and thus, there may be regional variations that were not fully assessed in this study. One may propose that brain regions particularly important to aging (e.g. hippocampus, occipital, and parietal) may demonstrate differential morphological changes compared to other regions. Thus, our study should be interpreted with these limitations in mind, and future work should be conducted to assess the generalizability of our results.

In conclusion, we found that CMBs – and the underlying pathological entity, CAA – do not correlate with traditional markers of neurodegenerative disease such as atrophy or cortical thinning. Instead, our results surprisingly indicate an association between CMBs and CAA and larger morphological brain measures.

WNL-2022-200395_sup1 ---http://links.lww.com/WNL/B854

WNL-2022-200395_coinvestigator_appendix 2 --- http://links.lww.com/WNL/B855

References:

1. Boyle PA, Yu L, Wilson RS, Leurgans SE, Schneider JA, Bennett DA. Person-specific contribution of neuropathologies to cognitive loss in old age. *Ann Neurol*. Jan 2018;83(1):74-83. doi:10.1002/ana.25123
2. Greenberg SM, Bacskai BJ, Hernandez-Guillamon M, Pruzin J, Sperling R, van Veluw SJ. Cerebral amyloid angiopathy and Alzheimer disease - one peptide, two pathways. *Nat Rev Neurol*. Jan 2020;16(1):30-42. doi:10.1038/s41582-019-0281-2
3. Haller S, Vernooij MW, Kuijer JPA, Larsson EM, Jager HR, Barkhof F. Cerebral Microbleeds: Imaging and Clinical Significance. *Radiology*. Apr 2018;287(1):11-28. doi:10.1148/radiol.2018170803
4. Poels MM, Vernooij MW, Ikram MA, et al. Prevalence and risk factors of cerebral microbleeds: an update of the Rotterdam scan study. *Stroke*. Oct 2010;41(10 Suppl):S103-6. doi:10.1161/STROKEAHA.110.595181
5. Romero JR, Preis SR, Beiser A, et al. Risk factors, stroke prevention treatments, and prevalence of cerebral microbleeds in the Framingham Heart Study. *Stroke*. May 2014;45(5):1492-4. doi:10.1161/STROKEAHA.114.004130
6. Viswanathan A, Greenberg SM. Cerebral amyloid angiopathy in the elderly. *Ann Neurol*. Dec 2011;70(6):871-80. doi:10.1002/ana.22516
7. Greenberg SM, Charidimou A. Diagnosis of Cerebral Amyloid Angiopathy: Evolution of the Boston Criteria. *Stroke*. Feb 2018;49(2):491-497. doi:10.1161/STROKEAHA.117.016990
8. Greenberg SM. Cerebral amyloid angiopathy: prospects for clinical diagnosis and treatment. *Neurology*. Sep 1998;51(3):690-4. doi:10.1212/wnl.51.3.690
9. Yates PA, Desmond PM, Phal PM, et al. Incidence of cerebral microbleeds in preclinical Alzheimer disease. *Neurology*. Apr 8 2014;82(14):1266-73. doi:10.1212/WNL.0000000000000285
10. Cordonnier C, van der Flier WM, Sluimer JD, Leys D, Barkhof F, Scheltens P. Prevalence and severity of microbleeds in a memory clinic setting. *Neurology*. May 9 2006;66(9):1356-60. doi:10.1212/01.wnl.0000210535.20297.ae
11. Goos JD, Kester MI, Barkhof F, et al. Patients with Alzheimer disease with multiple microbleeds: relation with cerebrospinal fluid biomarkers and cognition. *Stroke*. Nov 2009;40(11):3455-60. doi:10.1161/STROKEAHA.109.558197
12. Henneman WJ, Sluimer JD, Cordonnier C, et al. MRI biomarkers of vascular damage and atrophy predicting mortality in a memory clinic population. *Stroke*. Feb 2009;40(2):492-8. doi:10.1161/STROKEAHA.108.516286
13. Sepehry AA, Lang D, Hsiung GY, Rauscher A. Prevalence of Brain Microbleeds in Alzheimer Disease: A Systematic Review and Meta-Analysis on the Influence of Neuroimaging Techniques. *AJNR Am J Neuroradiol*. Feb 2016;37(2):215-22. doi:10.3174/ajnr.A4525
14. Brenowitz WD, Nelson PT, Besser LM, Heller KB, Kukull WA. Cerebral amyloid angiopathy and its co-occurrence with Alzheimer's disease and other cerebrovascular neuropathologic changes. *Neurobiol Aging*. Oct 2015;36(10):2702-8. doi:10.1016/j.neurobiolaging.2015.06.028

15. Karas GB, Burton EJ, Rombouts SA, et al. A comprehensive study of gray matter loss in patients with Alzheimer's disease using optimized voxel-based morphometry. *Neuroimage*. Apr 2003;18(4):895-907. doi:10.1016/s1053-8119(03)00041-7
16. Nitkunan A, Lanfranconi S, Charlton RA, Barrick TR, Markus HS. Brain atrophy and cerebral small vessel disease: a prospective follow-up study. *Stroke*. Jan 2011;42(1):133-8. doi:10.1161/STROKEAHA.110.594267
17. De Guio F, Duering M, Fazekas F, et al. Brain atrophy in cerebral small vessel diseases: Extent, consequences, technical limitations and perspectives: The HARNESS initiative. *J Cereb Blood Flow Metab*. Feb 2020;40(2):231-245. doi:10.1177/0271678X19888967
18. Fotiadis P, van Rooden S, van der Grond J, et al. Cortical atrophy in patients with cerebral amyloid angiopathy: a case-control study. *Lancet Neurol*. Jul 2016;15(8):811-819. doi:10.1016/S1474-4422(16)30030-8
19. Wang PN, Chou KH, Peng LN, et al. Strictly Lobar Cerebral Microbleeds Are Associated with Increased White Matter Volume. *Transl Stroke Res*. Feb 2020;11(1):29-38. doi:10.1007/s12975-019-00704-z
20. Graff-Radford J, Simino J, Kantarci K, et al. Neuroimaging Correlates of Cerebral Microbleeds: The ARIC Study (Atherosclerosis Risk in Communities). *Stroke*. Nov 2017;48(11):2964-2972. doi:10.1161/STROKEAHA.117.018336
21. Fotiadis P, Reijmer YD, Van Veluw SJ, et al. White matter atrophy in cerebral amyloid angiopathy. *Neurology*. Aug 4 2020;95(5):e554-e562. doi:10.1212/WNL.0000000000010017
22. Boden-Albala B, Cammack S, Chong J, et al. Diabetes, fasting glucose levels, and risk of ischemic stroke and vascular events: findings from the Northern Manhattan Study (NOMAS). *Diabetes Care*. Jun 2008;31(6):1132-7. doi:10.2337/dc07-0797
23. Gutierrez J, Elkind MS, Cheung K, Rundek T, Sacco RL, Wright CB. Pulsatile and steady components of blood pressure and subclinical cerebrovascular disease: the Northern Manhattan Study. *J Hypertens*. Oct 2015;33(10):2115-22. doi:10.1097/HJH.0000000000000686
24. Gutierrez J, Elkind MSV, Dong C, et al. Brain Perivascular Spaces as Biomarkers of Vascular Risk: Results from the Northern Manhattan Study. *AJNR Am J Neuroradiol*. May 2017;38(5):862-867. doi:10.3174/ajnr.A5129
25. Weiner MW, Veitch DP, Aisen PS, et al. The Alzheimer's Disease Neuroimaging Initiative: a review of papers published since its inception. *Alzheimers Dement*. Sep 2013;9(5):e111-94. doi:10.1016/j.jalz.2013.05.1769
26. Landau SM, Mintun MA, Joshi AD, et al. Amyloid deposition, hypometabolism, and longitudinal cognitive decline. *Ann Neurol*. Oct 2012;72(4):578-86. doi:10.1002/ana.23650
27. Tan B, Venketasubramanian N, Vrooman H, et al. Haemoglobin, magnetic resonance imaging markers and cognition: a subsample of population-based study. *Alzheimers Res Ther*. Nov 6 2018;10(1):114. doi:10.1186/s13195-018-0440-5
28. Gutierrez J, Menshawy K, Gonzalez M, et al. Brain large artery inflammation associated with HIV and large artery remodeling. *AIDS*. Jan 28 2016;30(3):415-23. doi:10.1097/QAD.0000000000000927
29. Gutierrez J, Rosoklija G, Murray J, et al. A quantitative perspective to the study of brain arterial remodeling of donors with and without HIV in the Brain Arterial Remodeling Study (BARS). *Front Physiol*. 2014;5:56. doi:10.3389/fphys.2014.00056
30. Cordonnier C, Potter GM, Jackson CA, et al. Improving interrater agreement about brain microbleeds: development of the Brain Observer MicroBleed Scale (BOMBS). *Stroke*. Jan 2009;40(1):94-9. doi:10.1161/STROKEAHA.108.526996

31. Dale AM, Fischl B, Sereno MI. Cortical surface-based analysis. I. Segmentation and surface reconstruction. *Neuroimage*. Feb 1999;9(2):179-94. doi:10.1006/nimg.1998.0395
32. Dong C, Nabizadeh N, Caunca M, et al. Cognitive correlates of white matter lesion load and brain atrophy: the Northern Manhattan Study. *Neurology*. Aug 4 2015;85(5):441-9. doi:10.1212/WNL.0000000000001716
33. Kantarci K, Gunter JL, Tosakulwong N, et al. Focal hemosiderin deposits and beta-amyloid load in the ADNI cohort. *Alzheimers Dement*. Oct 2013;9(5 Suppl):S116-23. doi:10.1016/j.jalz.2012.10.011
34. Vonsattel JP, Del Amaya MP, Keller CE. Twenty-first century brain banking. Processing brains for research: the Columbia University methods. *Acta Neuropathol*. May 2008;115(5):509-32. doi:10.1007/s00401-007-0311-9
35. Gyanwali B, Shaik MA, Tan CS, et al. Mixed-location cerebral microbleeds as a biomarker of neurodegeneration in a memory clinic population. *Aging (Albany NY)*. Nov 25 2019;11(22):10581-10596. doi:10.18632/aging.102478
36. Hilal S, Mok V, Youn YC, Wong A, Ikram MK, Chen CL. Prevalence, risk factors and consequences of cerebral small vessel diseases: data from three Asian countries. *J Neurol Neurosurg Psychiatry*. Aug 2017;88(8):669-674. doi:10.1136/jnnp-2016-315324
37. Farrall AJ, Wardlaw JM. Blood-brain barrier: ageing and microvascular disease--systematic review and meta-analysis. *Neurobiol Aging*. Mar 2009;30(3):337-52. doi:10.1016/j.neurobiolaging.2007.07.015
38. Tsai HH, Tsai LK, Chen YF, et al. Correlation of Cerebral Microbleed Distribution to Amyloid Burden in Patients with Primary Intracerebral Hemorrhage. *Sci Rep*. Mar 17 2017;7:44715. doi:10.1038/srep44715
39. Sveinbjornsdottir S, Sigurdsson S, Aspelund T, et al. Cerebral microbleeds in the population based AGES-Reykjavik study: prevalence and location. *J Neurol Neurosurg Psychiatry*. Sep 2008;79(9):1002-6. doi:10.1136/jnnp.2007.121913
40. Kovari E, Charidimou A, Herrmann FR, Giannakopoulos P, Bouras C, Gold G. No neuropathological evidence for a direct topographical relation between microbleeds and cerebral amyloid angiopathy. *Acta Neuropathol Commun*. Aug 14 2015;3:49. doi:10.1186/s40478-015-0228-9
41. Kovari E, Herrmann FR, Hof PR, Bouras C. The relationship between cerebral amyloid angiopathy and cortical microinfarcts in brain ageing and Alzheimer's disease. *Neuropathol Appl Neurobiol*. Aug 2013;39(5):498-509. doi:10.1111/nan.12003
42. Reijmer YD, Fotiadis P, Riley GA, et al. Progression of Brain Network Alterations in Cerebral Amyloid Angiopathy. *Stroke*. Oct 2016;47(10):2470-5. doi:10.1161/STROKEAHA.116.014337
43. Iliff JJ, Wang M, Liao Y, et al. A paravascular pathway facilitates CSF flow through the brain parenchyma and the clearance of interstitial solutes, including amyloid beta. *Sci Transl Med*. Aug 15 2012;4(147):147ra111. doi:10.1126/scitranslmed.3003748
44. Hadaczek P, Yamashita Y, Mirek H, et al. The "perivascular pump" driven by arterial pulsation is a powerful mechanism for the distribution of therapeutic molecules within the brain. *Mol Ther*. Jul 2006;14(1):69-78. doi:10.1016/j.ymthe.2006.02.018
45. Mestre H, Tithof J, Du T, et al. Flow of cerebrospinal fluid is driven by arterial pulsations and is reduced in hypertension. *Nat Commun*. Nov 19 2018;9(1):4878. doi:10.1038/s41467-018-07318-3

46. Mestre H, Du T, Sweeney AM, et al. Cerebrospinal fluid influx drives acute ischemic tissue swelling. *Science*. Mar 13 2020;367(6483)doi:10.1126/science.aax7171
47. van Veluw SJ, Hou SS, Calvo-Rodriguez M, et al. Vasomotion as a Driving Force for Paravascular Clearance in the Awake Mouse Brain. *Neuron*. Feb 5 2020;105(3):549-561 e5. doi:10.1016/j.neuron.2019.10.033
48. Weller RO, Subash M, Preston SD, Mazanti I, Carare RO. Perivascular drainage of amyloid-beta peptides from the brain and its failure in cerebral amyloid angiopathy and Alzheimer's disease. *Brain Pathol*. Apr 2008;18(2):253-66. doi:10.1111/j.1750-3639.2008.00133.x
49. Haller S, Montandon ML, Lazeyras F, et al. Radiologic-Histopathologic Correlation of Cerebral Microbleeds Using Pre-Mortem and Post-Mortem MRI. *PLoS One*. 2016;11(12):e0167743. doi:10.1371/journal.pone.0167743
50. Shams S, Martola J, Cavallin L, et al. SWI or T2*: which MRI sequence to use in the detection of cerebral microbleeds? The Karolinska Imaging Dementia Study. *AJNR Am J Neuroradiol*. Jun 2015;36(6):1089-95. doi:10.3174/ajnr.A4248

Table 1: Baseline Demographic Characteristics				
	NOMAS N = 918	ADNI N=1017	EDIS N=722	BARS N=82
Age, yr, mean (SD)	70 (9)	73 (7)	70 (7)	81 (11)
Women, n (%)	573 (62)	500 (51)	359 (50)	38 (46)
Race/ethnicity				
Non-Hispanic white, n (%)	161 (18)	908 (89)	-	61 (74)
Non-Hispanic black, n (%)	147 (16)	42 (4)	-	8 (10)
Hispanic, n (%)	610 (66)	35 (3)	-	12 (16)
Chinese, n (%)	-	-	223 (31)	-
Indian, n (%)	-	-	259 (36)	-
Malay, n (%)	-	-	240 (33)	-
Apoe4 carriers, n (%)	204 (23)	428 (42)	122 (17)	11 (41)*
Hypertension, n (%)	707 (77)	537 (53)	576 (80)	42 (51)
Diabetes, n (%)	221 (24)	124 (12)	258 (36)	10 (12)
Hypercholesterolemia, n (%)	744 (81)	581 (57)	549 (76)	30 (37)
Current smoker, n (%)	89 (10)	18 (2)	197 (27)	14 (17)
Any CMB (CAA for BARS), n (%)	61 (6)	228 (22)	223 (31)	64 (78)
Lobar	36 (4)	188 (19)	208 (27)	55 (67)
Deep (basal ganglia/brain stem)	25 (3)	77 (8)	124 (16)	39 (48)
Brain infarcts, n (%)	137 (15)	36 (4)†	110 (17)	33 (40)
Mean cortical thickness, mm, (SD)	2.29 (0.10)	2.46 (0.13)	2.37 (0.11)	2.57 (0.27)

Abbreviations: NOMAS = Northern Manhattan Study, BARS = Brain Arterial Remodeling Study, ADNI = Alzheimer's Disease Neuroimaging Initiative, EDIS = Epidemiology of Dementia in Singapore study, *Apoe* = apolipoprotein E
*Only available in 27 cases
†Data on brain infarcts from ADNI is missing; self-reported history of stroke was used as a surrogate.

Table 2: Associations between CMB by anatomical location and severity with brain volumetric measures and cortical thickness.

			Total brain volume	Gray matter volume	White matter volume	Cortical thickness (in microns)
			Log transformed			
			Beta estimates ± standard error			
			NOMAS			
Model 1		Any CMB	10.06 ± 5.07	7.54 ± 5.64	19.31 ± 8.33	8.43 ± 11.99
Model 2		Superficial CMB	11.99 ± 6.63*	7.10 ± 1.38	31.92 ± 10.87†	11.28 ± 15.66
		Deep CMB	-1.81 ± 7.67	12.70 ± 5.58	1.85 ± 12.64	15.40 ± 18.21
Model 3	Superficial	No CMB	Reference			
		One CMB	11.96 ± 7.95	4.82 ± 8.73	20.40 ±12.80	16.8 ± 18.57
		≥ two CMB	6.31 ± 11.78	2.87 ± 14.24	54.47 ± 20.91†	-17.38 ± 30.27
	Deep	No CMB	Reference			
		One CMB	8.17 ± 6.93	10.73 ± 7.68	4.32 ± 11.28	13.43 ± 16.34
		≥ two CMB	17.27 ± 11.49	7.94 ± 24.35	19.88 ± 35.76	-57.52 ± 51.76
			ADNI			
Model 1		Any CMB	2.75 ± 2.32	0.59 ± 2.92	6.15 ± 4.78	14.9 ± 10.1
Model 2		Superficial CMB	1.57 ± 2.58	-2.52 ± 3.25	7.12 ± 5.32	8.3 ± 11.2
		Deep CMB	4.55 ± 3.59	7.0 ± 4.552	3.03 ± 7.38	13.5 ± 16.4
Model 3	Superficial	No CMB	Reference			
		One CMB	2.67 ± 3.01	-3.56 ± 3.79	9.28 ± 6.19	17.31 ± 12.8
		≥ two CMB	-2.25 ± 1.46	-0.77 ± 5.25	-0.37 ± 8.56	-12.7 ± 18.40
	Deep	No CMB	Reference			
		One CMB	1.64 ± 3.92	5.87 ± 4.94	-2.64 ± 8.07	14.34 ± 17.35
		≥ two CMB	20.30 ± 1.91†	10.10 ± 9.97	33.77 ± 16.27†	28.84 ± 39.30
			EDIS (Singapore)			
Model 1		Any CMB	-0.06 ± 1.16	-1.14 ± 2.29	3.02 ± 2.18	-11.13 ± 8.17
Model 2		Superficial CMB	0.11 ± 1.25	0.20 ± 2.47	2.96 ± 2.36	-1.86 ± 8.82
		Deep CMB	-1.39 ± 1.58	-3.99 ± 3.12	-0.38 ± 2.96	-13.87 ± 11.15
Model 3	Superficial	No CMB	Reference			
		One CMB	1.50 ± 1.46	1.41 ± 2.90	3.65 ± 2.76	7.01 ± 14.01
		≥ two CMBs	-2.83 ± 2.00	-1.98 ± 3.96	0.71 ± 3.78	-4.73 ± 10.38
	Deep	No CMB	Reference			
		One CMB	-1.16 ± 1.79	-3.31 ± 3.56	-1.26 ± 3.36	-7.8 ± 12.69
		≥ two CMB	0.49 ±2.86	-3.19 ± 5.67	2.40 ± 5.38	-34.63 ± 20.22

Analytic notes: Models adjusted age, sex, race/ethnicity, *Apoe*4, head size, prevalence of hypertension, diabetes, hypercholesterolemia, smoking, MRI evidence of infarction, and total white matter hyperintensity volume.

*=P value 0.10-0.05; †=P value < 0.05

Table 3: Associations between CMB by anatomical location and severity with brain volumetric measures and cortical thickness.

			Total brain volume	Gray matter volume	White matter volume	Cortical thickness (in microns)
			Log transformed			
			Beta estimates ± standard error			
			META-ANALYSIS (United States)			
Model 1		Any CMB	4.02 ± 2.11	2.06 ± 2.59	9.41 ± 4.14†	12.21 ± 7.72
Model 2		Superficial CMB	2.94 ± 2.41	5.63 ± 1.27†	11.91 ± 4.77†	9.31 ± 9.11
		Deep CMB	3.41 ± 3.25	9.27 ± 3.52†	2.73 ± 6.37	14.35 ± 12.19
Model 3	Superficial	No CMB	Reference			
		One CMB	10.19 ± 6.59	-2.23 ± 3.47	11.38 ± 5.57†	17.14 ± 10.54*
		≥ two CMB	-2.12 ± 1.45	-0.33 ± 4.92	7.50 ± 7.92	-13.96 ± 15.72
	Deep	No CMB	Reference			
		One CMB	3.22 ± 3.41	7.29 ± 4.15*	-0.28 ± 6.56	13.86 ± 11.89
		≥ two CMB	20.21 ± 1.88†	9.79 ± 9.23	31.38 ± 14.8†	-2.74 ± 31.3
			META-ANALYSIS (All 3 Cohorts)			
Model 1		Any CMB	0.89 ± 1.02	0.26 ± 1.72	4.4 ± 1.93†	1.2 ± 5.61
Model 2		Superficial CMB	0.71 ± 1.11	4.49 ± 1.13†	4.72 ± 2.11†	3.54 ± 6.34
		Deep CMB	-0.47 ± 1.42	1.84 ± 2.34	0.17 ± 2.68	-1.01 ± 8.22
Model 3	Superficial	No CMB	Reference			
		One CMB	1.99 ± 1.3	-0.08 ± 2.22	5.17 ± 2.47†	13.48 ± 8.42
		≥ two CMBs	-2.36 ± 1.17†	-1.33 ± 3.09	1.97 ± 3.41	-7.53 ± 8.66
	Deep	No CMB	Reference			
		One CMB	-0.21 ± 1.58	1.18 ± 2.7	-1.06 ± 2.99	3.73 ± 8.68
		≥ two CMB	14.25 ± 1.57†	0.37 ± 4.83	5.78 ± 5.06	-25.24 ± 16.98

Analytic notes: Models adjusted for age, sex, race/ethnicity, apoe4, head size, prevalence of hypertension, diabetes, hypercholesterolemia, smoking, MRI evidence of infarction, and total white matter hyperintensity volume.
*=P value 0.10-0.05
†=P value < 0.05

FIGURE LEGENDS

FIGURE 1: Example vessels with cerebral amyloid angiopathy (CAA) and their anatomical distribution. (A) “Double barrel” appearance of CAA in the frontal cortex showing detachment and delamination of the outer part of the tunica media. Many neuritic plaques observed in surrounding tissue. (B) Copious vessels affected by CAA noted in the leptomeningeal space of the frontal cortex. (C) CAA vessels observed in the caudate nucleus. (D) CAA vessel observed in the globus pallidus. (E)

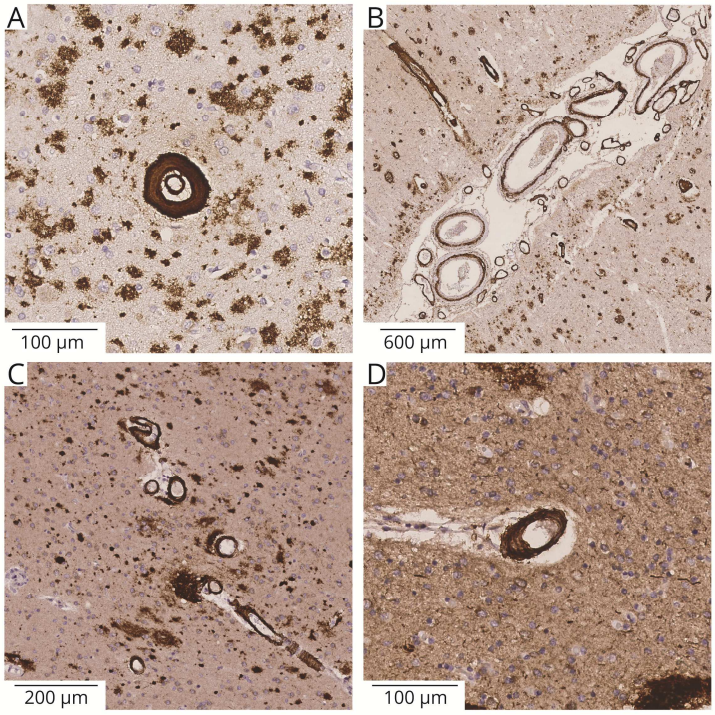

FIGURE 2: The mean prevalence of CMB by age and anatomical location for the three cohorts. Age is discretized into 5-year increments. (1) Blue indicates any CMB; (2) Red indicates superficial (or lobar) CMBs (i.e. cortical or adjacent subcortical white matter); and (3) Green indicates deep (basal ganglia, brain stem or cerebellar nuclei) CMBs. The prevalence of CMBs was significantly associated with age in NOMAS (OR=1.035, 1.008-1.063), ADNI (OR=1.040, 1.021-1.059), and EDIS (OR=1.036, 1.008-1.064) cohorts. Abbreviations: NOMAS = Northern Manhattan Study, BARS = Brain Arterial Remodeling Study, ADNI = Alzheimer's Disease Neuroimaging Initiative, EDIS = Epidemiology of Dementia in Singapore study, OR = Odds Ratio.

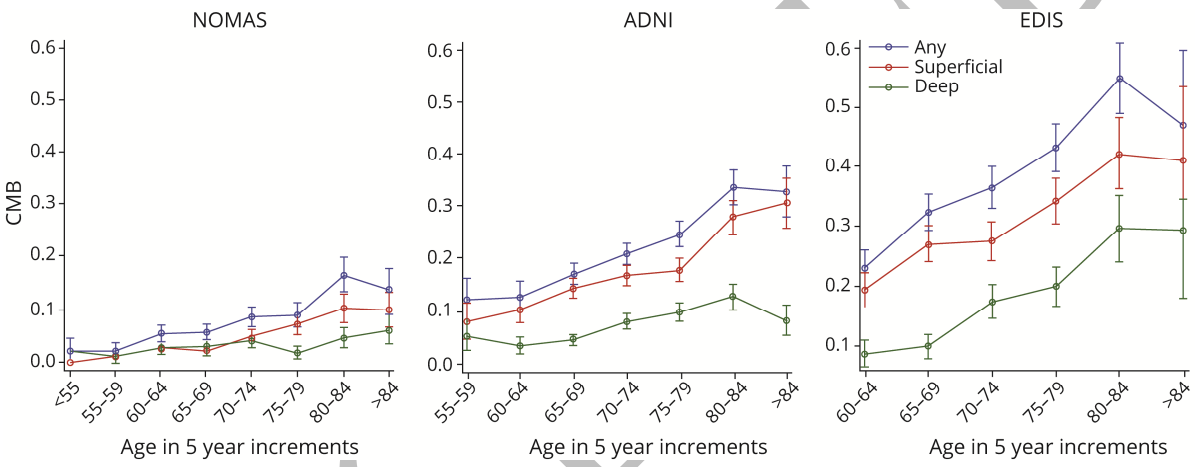

FIGURE 3: The mean of cerebral amyloid angiopathy (CAA) CAA number of vessels per 40 μm^2 in the BARS cohort. The gray matter areas seen in the caudate, internal capsule, globus pallidus, and thalamus were excluded from the "Cortical" and "Extra-Cortical" columns and represented instead under the "Subcortical" column. BARS = Brain Arterial Remodeling Study.